
# Università degli Studi di Padova

**Dipartimento di Fisica e Astronomia "Galileo Galilei**

**Corso di Laurea in Astronomia**


**Tesi di Laurea**

# The fundamental plane at different cosmic epochs with the EAGLE simulation


**Relatore:**
**Mauro D'Onofrio**

**Laureando:**
**Franesco Brevi**



**Anno Accademico 2023/2024**

**Abstract**

In this thesis, data from the EAGLE project has been utilised to study the dependence on time of the fundamental plane qualitatively; the tight relation between early-type galaxies' size, surface brightness and velocity dispersion. What has been found is that the plane changes its slope as time passes while the scatter remains unchanged around $\sim 0.1$ even at $z = 4$. Moreover, the trend isn't the same for every galaxy, indeed the most massive ones depart from the others following a steeper slope only after a redshift between $1 < z < 2$. This is well appreciable even in the $I_e - R_e$ plane, where the massive galaxies evolve linearly near the zone of exclusion's (ZoE) boundary. Instead, the others, begin to distribute in a cloud starting before $z = 1$, defining the typical curvature visible at lower redshifts on the plane.

**Sommario**

In questa tesi sono stati utilizzati i dati del progetto EAGLE per studiare qalitativamente la dipendanza dal tempo del piano fondamentale; la stretta relazione tra la dimensione, la brillanza superficiale e la dispersione di velocità delle galassie early-type. E' stato trovato che il piano cambia pendenza al passare del tempo, mentre la sua dispersione rimane pressochè invariata attorno a $\sim 0.1$ anche a $z = 4$. Si è anche osservato che le galassie massicce iniziano a distribuirsi con una pendenza maggiore rispetto alle altre a partire da un redshift compreso tra $1 < z < 2$ Questo andamento è visibile anche dal piano $I_e - R_e$ nel quale le galassie più massicce si muovono, con una dispersione lineare, lungo il confine con la zona di esclusione. Invece le altre, di distribuiscono in unaa nuvola prima di $z = 1$, iniziando a definire la tipica curvatura che è visibile sul piano a redshift inferiori.

# Contents

**1 Introduction** **1**

**2 The EAGLE simulation** **2**
2.1 Galaxies in the Eagle simulation . . . . . 2
2.2 Sample selection . . . . . 3
2.3 Non-homology of the sample . . . . . 3
2.4 Comparison with the Illustris simulation . . . . . 4

**3 The fundamental plane** **5**
3.1 Separation of ETGs from LTGs by colour . . . . . 5
3.2 Temporal evolution of the FP . . . . . 8
3.3 Ie - Re plane . . . . . 9
3.4 Faber-Jackson diagram . . . . . 11
3.5 Comparison with virial theorem . . . . . 13

**4 Conclusion** **14**

**5 Acknowledgment** **15**

# 1 Introduction

It has been seen that in the three-dimensional parameter space; half-light radius ($R_e$), central velocity dispersion ($\sigma$), and mean surface brightness within Re ($I_e$), early-type galaxies (ETGs) distribute on a plane, known as the fundamental plane (FP) (e.g. Djorgovski & Davis 1987 [1]; Dressler et al. 1987 [2]), with a very little scatter and it can be written as follows:

$$logR_e = a\ log\sigma + b\ logI_e + c \tag{1}$$

where the coefficients a, b, and c are the slope and the zero-point of the plane respectively.

From a physical point of view, the FP has always been associated with the virial theorem which would lead to a value of the constants of $a = 2$ and $b = -1$, but the observational data lead to other values like $a \sim 1.2$ and $b \sim -0.8$.
This has been known as the problem of the FP tilt (e.g., Faber et al. 1987 [3]; Ciotti 1991 [4]; Jorgensen et al. 1996 [5]; Cappellari et al. 2006 [6]; D'Onofrio et al. 2006 [7]; Bolton et al. 2007 [8]). The actual reason for this tilt is still unknown, but some of the causes that seem to explain it, at least partially, are:

- the existence of structural and dynamical nonhomology in the stellar systems (see e.g., Prugniel & Simien 1997 [9]; Busarello et al. 1998 [10]; Trujillo et al. 2004 [11]; D'Onofrio et al. 2008 [12]),
- a progressive change in the stellar mass-to-light ratio $M_*/L$ along the plane (Faber et al. 1987 [3]; van Dokkum & Franx 1996 [13]; Cappellari et al. 2006 [6]; Holden et al. 2010 [14]; de Graaff et al. 2021 [15]),
- the dark matter content (Ciotti et al. 1996 [16]; Borriello et al. 2003 [17]; Tortora et al. 2009 [18]; de Graaff et al. 2021 [15]).

Moreover, some studies discussed about a possible curvature of the FP (Jorgensen et al. 1996 [5]; Zaritsky et al. 2006 [19]; D'Onofrio et al. 2008 [12]; Hyde & Bernardi 2009b [20]) and Yoon & Park (2022) [21] arrived at the conclusion that the FP is a slightly curved and twisted surface.

From its discovery, the FP, has found numerous astrophysical applications serving as a distance indicator (e.g., D'Onofrio et al. 1997 [22]), a diagnostic tool for galaxy evolution (e.g., van Dokkum & Franx 1996 [13]; van Dokkum & van der Marel 2007 [23]; Holden et al. 2010 [14]) and for mapping the peculiar velocity field (e.g., Willick et al. 1995 [24]; Strauss & Willick 1995 [25]).

Unluckily, at a redshift higher than 0.7, observational data become difficult to obtain and so the FP extrapolated becomes more and more unreliable as z grows. Then hydrodynamical simulations like EAGLE, come in handy because they can give us an idea of what could be observed in the future with telescopes as big as the ELT.
Therefore, this work aims to estimate the dependence of the FP on redshift calculating it at $z = 0,\ 0.1,\ 1,\ 2,\ 3$ and 4, using data from the EAGLE simulation and at the same time, analyse the change of slope that occurs for massive galaxies.

# 2 The EAGLE simulation

The Evolution and Assembly of Galaxies and their Environments, also known as EAGLE, is a suite of cosmological, hydrodynamic simulations of a standard $\Lambda$ cold dark matter universe (described in detail by Schaye et al. 2015 [26], and Crain et al. 2015 [27]), whit cosmological parameters inferred from the Planck Collaboration I and XVI (2014): $\Omega_m = 0.307$, $\Omega_b = 0.04825$, $\Omega_\Lambda = 0.693$ and $H_0 = 100\ h\ km\ s^{-1}\ Mpc^{-1}$, where $h = 0.6777$.
Where $\Omega_m$, $\Omega_b$ and $\Omega_\Lambda$ are the average densities of matter, baryonic matter and dark energy in units of the critical density at redshift zero.

The initial conditions were generated at z = 127 using second-order Lagrangian perturbation theory (Jenkins 2010 [28]) and then evolved using a modified version of the N-body tree smoothed particle hydrodynamics (SPH) code GADGET-3 (Springel 2005 [29]). One of the modifications is the addiction of subgrid models to govern processes occurring on scales below the resolution limit of the simulations like; the radiative cooling (Wiersma, Schaye & Smith 2009a [30]), the star formation (Schaye & Dalla Vecchia 2008 [31]), stellar mass loss (Wiersma et al. 2009b [32]), energetic feedback from star formation (Dalla Vecchia & Schaye 2012 [33]), black hole accretion, merging and feedback (Rosas-Guevara et al. 2015 [34]; Schaye et al. 2015 [26]). The efficiency of the stellar feedback and black hole accretion have been calibrated to the observed $z = 0.1$ galaxy stellar mass function (GMSF) and galaxy size distribution.

For this work it has been used the intermediate-resolution simulation REF-L100N1504. It follows $2\times1504^3$ particles in a cubic volume of 100 comoving Mpc (cMpc) on a side from redshift $z = 127$ to the present day (S. McAlpine et al. 2016 [35]) . This corresponds to an equal number of baryonic and dark matter particles with initial mass $m_{gas} = 1.81 \times 10^6\ M_\odot$ and $m_{DM} = 9.70 \times 10^6\ M_\odot$ per particle. The simulation uses a Plummer-equivalent gravitational softening length of $\epsilon = 2.66\ ckpc$ for $z > 2.8$ and $\epsilon = 0.7\ pkpc$ (proper kpc) for $z < 2.8$, but in this work, galaxies with a radius smaller than the sensitivity will be considered anyway to qualitatively show their trends on the fundamental plane.

## 2.1 Galaxies in the Eagle simulation

In the EAGLE simulations, galaxies, are identified by the SUBFIND algorithm (Springel et al. 2001 [36]; Dolag et al. 2009 [37]) which select gravitationally bound substructures (subhaloes) in haloes, found by running the friends-of-friends (FoF; Davis et al. 1985 [38]) algorithm on the dark matter particles with linking length 0.2 times the mean interparticle separation. The subhalo that contains the particle with the lowest value of the gravitational potential of the FoF halo, is defined as the central galaxy while the other subhaloes are classified as satellite galaxies (Schaye et al. 2015 [26]).

The galaxy's properties have been calculated taking into consideration all the particles associated at the subhalo, but instead, for the absolute magnitude in different bands, only the particles within a spherical aperture of radius 30 pkpc are considered. Therefore, the size of the aperture may affect the position of high massive galaxies ($M_* < 10^{11}\ M_\odot$) in the FP, but the aim of this work is limited to observing whether there is a dependence of the FP on z, for this reason, the previous statement will be disregarded from now on.

## 2.2 Sample selection

For this work, it has been decided to follow the evolution of the FP for a specific set of galaxies along an interval of redshift spanning between $0 \leqslant z \leqslant 4$. More precisely, the FP has been calculated for six values of z, $z = 0,\ 0.1,\ 1,\ 2,\ 3,\ 4$.

To trace the evolution of individual galaxies along this time, galaxy merger trees, built by tracing the most bound particles of each subhalo along consecutive snapshots (redshifts), have been used. This allows determining all the progenitors of the galaxies at $z = 0$, but for the purpose of this work, only the main progenitor branch, the one with the largest branch mass (DeLucia & Blaizot 2007), have been considered.
Hypothesizing that the main branch describes the same galaxy at different epochs, it is possible to determine the properties of the latter at different redshifts. Using this supposition, the sample of galaxies has been selected so that all galaxies already had a stellar mass $M > 10^{8.5}\ M_{\odot}$ at $z = 4$ and this limit its size to a total number of 2413 galaxies.

## 2.3 Non-homology of the sample

For a long time, it has been believed that all ETGs had the same Sèrsic index $n = 4$ until their non-homology was demonstrated by D'Onofrio et al. 2008 [12]. From that moment, part of the FP tilt could be explained by the non-homology instead of a systematic change in the $M/L$ ratio as it has been believed since then. In the EAGLE database, the Sèrsic indexes are available at $z = 0.1$ for galaxies with a stellar mass $M > 10^{10}\ M_{\odot}$, and they have been compared with a WINGS's (WIde-field Nearby Galaxy-cluster Survey) sample of 261 ETGs, provided by the supervisor, in Fig. 1. For the realisation of these diagrams, only ETGs galaxies have been taken into consideration from the EAGLE's data sample, and they were selected as those with a colour index $g - r > 0.62$, as explained in Sec. 3.1, and a Sèrsic index $n > 2$. As the galaxies distribute with a high scatter on the planes, an orthogonal regression was utilised to make the relation between the variables more appreciable. As one can observe in Fig. 1, the EAGLE simulation naturally generates a non-homologous sample of ETGs, that follow quite well the observational data on the $L - n$ plane, While on the $R_e - n$ diagram, the simulation deviates from the observed data. In Tab. 1, are reported the slopes of the orthogonal fits showed in Fig.1.

| | $L-n$ | | | $R-n$ | | |
|---|---|---|---|---|---|---|
| | m | d | $\chi^2$ | m | d | $\chi^2$ |
| EAGLE | 0.16 | -1.18 | 0.0159 | 0.09 | 0.40 | 0.0177 |
| WINGS | 0.18 | -1.26 | 0.0167 | 0.29 | 0.39 | 0.0152 |

**Table 1:** In the table are reported the values of the slope and intercept of the lines in Fig. 1 with their related reduced $\chi^2$

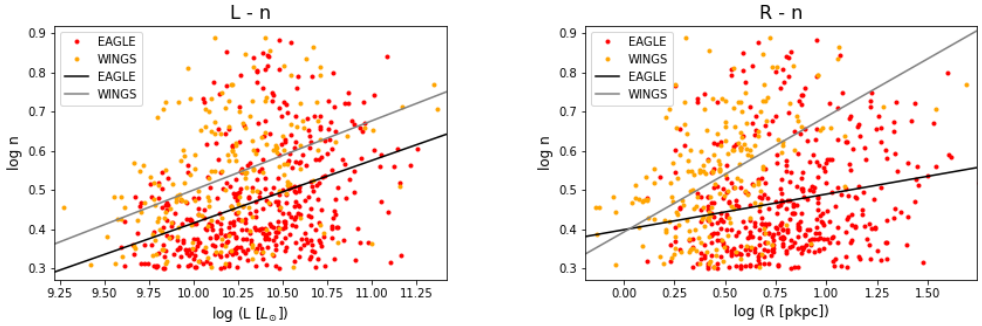


**(a)** **(b)**

**Figure 1:** In the diagrams have been compared only early-type galaxies from the WINGS survey, in orange, and the EAGle simulation, in red. The two lines are the orthogonal fit, grey for WINGS' data and black for the EAGLE. On the left, the $logL - logn$ relation is displayed while on the right, the $logR - logn$ one.

## 2.4 Comparison with the Illustris simulation

The IllusstrisTNG project is a suite of cosmological, gravomagneto-hydrodynamical simulations of galaxy formation that attempt to reproduce the universe as it is observed. One of its simulations is TNG100 which works in a cubic volume of 75 cMpc per side (Naiman et al. 2018 [39]; Springel et al. 2017 [40]; Marinacci et al. 2018 [41]; Pillepich et al. 2017 [42]; Nelson at al. 2017 [43]), a little smaller than the one considered from the EAGLE project (100 cMpc per side), but they share a similar resolution. The TNG100 simulation adopt $\Omega_{\Lambda,0} = 0.6911$, $\Omega_{m,0} = 0.3089$, $\Omega_{b,0} = 0.0486$, and $h = 0.6774$ as cosmological constants. The relation between stellar mass and half stellar mass radius of the two simulations are compared in Fig. 2, and a certain resemblance can be observed. Therefore, one can expect similar results, as the ones found in this work, analysing the TNG100 simulation's data.

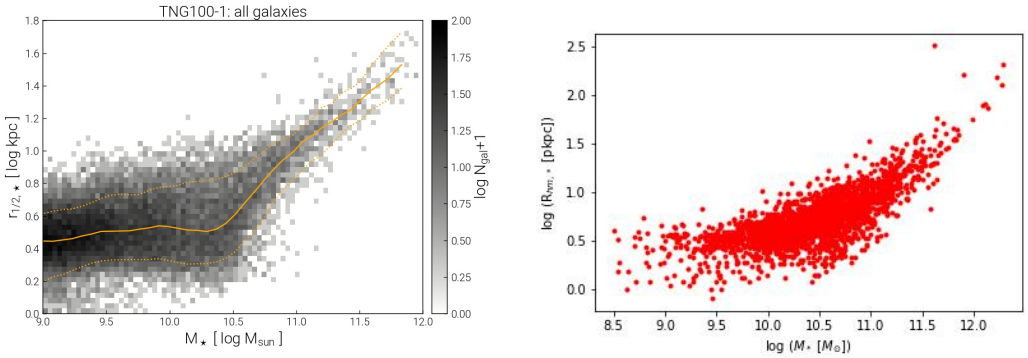


**(a)** **(b)**

**Figure 2:** Here are displayed the half stellar mass radius and stellar mass relations for the IllustrisTNG100 sample on the left, and the EAGLE sample on the right.

# 3 The fundamental plane

The FP is a two-dimensional surface in the three-dimensional parameter space: half-light radius ($R_e$), central velocity dispersion ($\sigma$) and mean surface brightness within Re ($I_e$).

The mass that is enclosed in the effective radius ($R_e$) may change depending on how the sizes of the galaxies have been measured, i.e. from the stellar mass or optical light distributions (de Graaff et al. 2022a [44]). The effects caused by different definitions are deeply discussed by de Graaff (2022b) [45]. For this work, it was chosen to define the sizes utilising the stellar mass, in particular, the half stellar mass radius ($R_{hm*}$) was picked instead of the effective radius ($R_e$).

From the EAGLE database, one can acquire the absolute magnitude, without dust attenuation, of the galaxies in different SDSS and UKIRT filters and for this work, it has been decided to calculate the mean surface brightness in the $r$ band allowing a possible comparison with observational data.
The mean surface brightness in the r band has been obtained by calculating first the luminosity:

$$L_r = 10^{-0.4(M_r - M_{\odot,r})} \tag{2}$$

where $M_r$ is the absolute magnitude of the galaxy in the r band and $M_{\odot,r} = 4.65$ is the solar one in the AB system and SDSS_r filter (Willmer 2018 [46]).
Then

$$I_{e,r} = \frac{L_r}{2\pi\ R^2_{hm,*}} \tag{3}$$

where $R_{hm*}$ is the half stellar mass radius in pc.

## 3.1 Separation of ETGs from LTGs by colour

It is important to clarify that the sample of galaxies described in section 2.2 includes galaxies of every morphology, even the late type ones (LTGs). However, it's known that the FP has very little scatter for ETGs. Therefore, the colour index $(g - r)$ of the entire sample has been studied in Fig. 3 to roughly select the early-type galaxies.

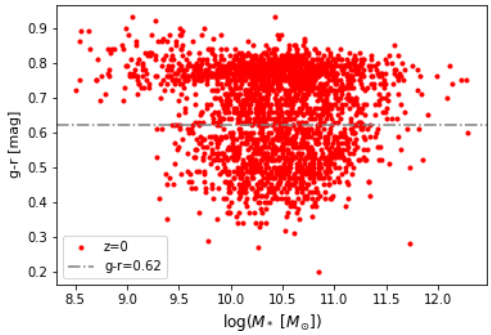


**Figure 3:** Here is displayed the relation of the stellar mass on the colour index $g-r$ for the EAGLE sample at $z=0$. It can be noticed that galaxies are distributed in two distinct groups, one redder, the ETGs, and one bluer, the LTGs.

One can see that at low redshift, the galaxies are mainly distributed in two groups, one redder with a mean colour of $g-r \sim 0.8$, and one bluer with a mean of $g-r \sim 0.5$ and they are quite well separated by the dashed line at $g-r=0.62$. A similar partition can be seen even in the work of Strateva et al. (2001) [47] where a large number of observed galaxies have been studied. Therefore, early-type galaxies at $z=0$ can be roughly defined as those with a colour index $g-r>0.62$. However, this method becomes inappropriate at higher redshift because, in the distant past, galaxies were more star-forming resulting in a generally bluer colour for every morphology.

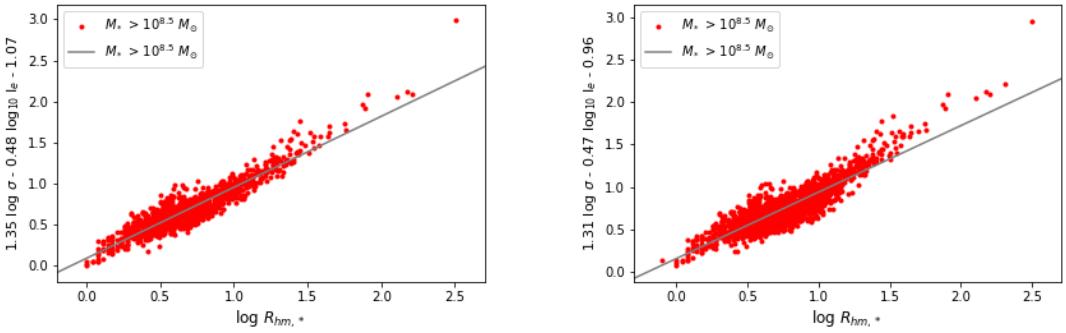


**Figure 4:** Here is displayed the fundamental plane at $z=0$ for the EAGLE simulation's sample. On the left: considering only the early-type galaxies. On the right: considering the totality of the sample. The grey lines are the least square fit.

In Fig. 4, the fundamental planes at $z=0$, considering the totality of the sample (left), and only the early-type galaxies selected as defined before (right), are compared. As one can see from Tab. 2, the coefficients of the two planes, $a$,

| | ETGs only | ETGs + LTGs |
|---|---|---|
| a | 1.35 ± 0.05 | 1.31 ± 0.05 |
| b | -0.48 ± 0.03 | -0.47 ± 0.03 |
| c | -1.07 ± 0.09 | -0.96 ± 0.12 |
| m | 0.86 ± 0.04 | 0.78 ± 0.04 |
| d | 0.09 ± 0.02 | 0.16± 0.03 |
| scatter | 0.10 | 0.11 |

**Table 2:** Here are reported the values of the fundamental planes constants $a$, $b$ and $c$ of Fig. 3, and also the slope, the intercept of the least square fit and the scatter of the galaxies from it.

$b$ and $c$, are compatible within the error. Therefore, in a first approximation, there isn't a significant difference between studying one plane or the other. For this reason, all the following reasoning will be made considering the totality of the sample. To estimate values and errors that one can find in Tab. 2, 200 galaxies were chosen randomly from the sample and the fundamental plane was computed for them. Then the process was repeated 400 times and their mean value and standard deviation have been reported in the table.

## 3.2 Temporal evolution of the FP

Taking into account what has been said before about the morphology of galaxies, in Fig. 5, one can see the fundamental plane at different redshifts and check the value of the three constants in Tab. 3. As one would expect from a model of a hierarchical universe, the plane evolves with time as the parameters change, but from Fig. 6 can be observed that massive galaxies evolve differently compared to the less massive ones. As can be seen, this difference begins at redshift $1 < z < 2$. One can compare the constants' values of the two groups at Tab. 3 and 4, and observe their evolution over time in Fig. 6.

It seems that the fundamental plane of the massive galaxies is more stable over time as its constants don't change as much as the ones for light galaxies. One particularity shown by the EAGLE simulation data is that even if the plane changes over time, the scatter remains around 0.1 even at redshifts $z = 4$. This was first observed by Sperello & Lanzoni (2006) [48] for a maximum redshift of $z = 1.3$.

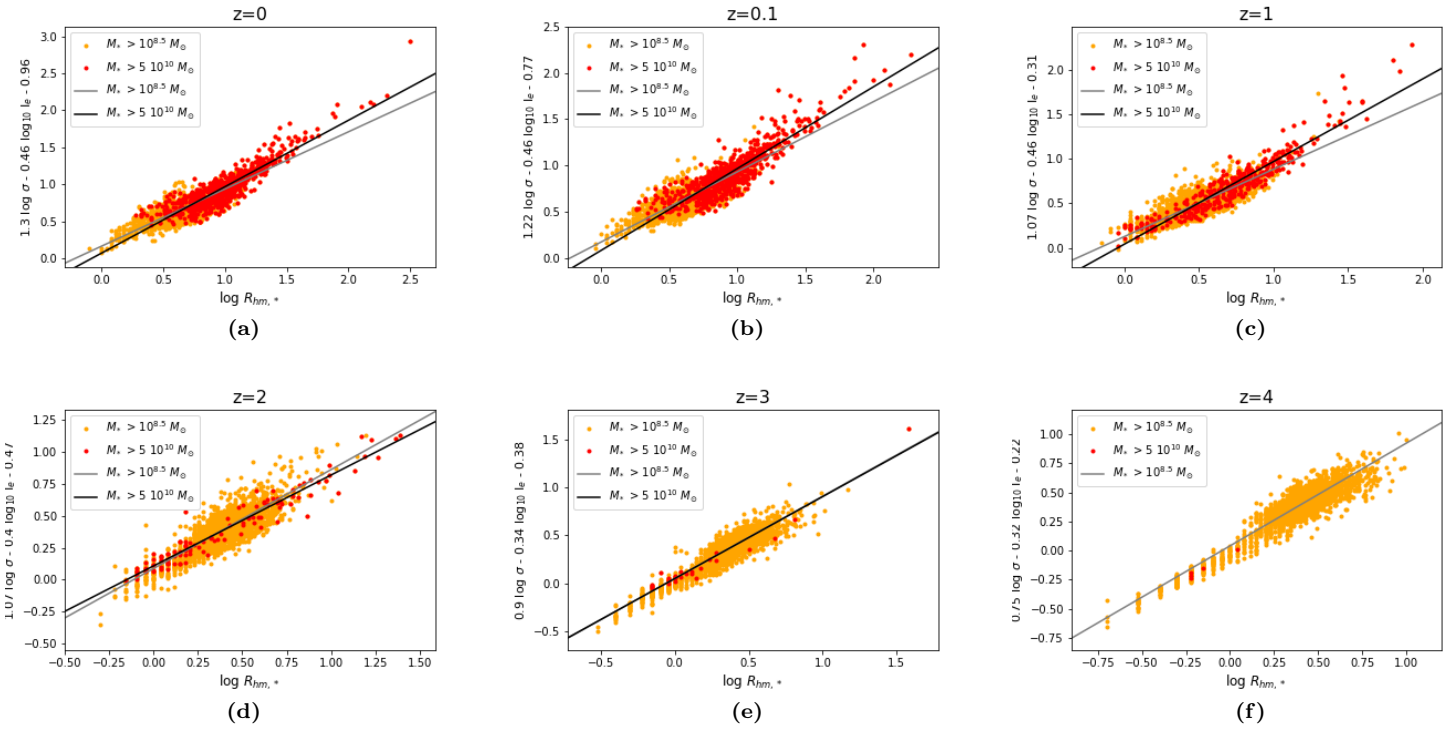


**Figure 5:** Here is displayed the fundamental plane as six different redshifts. Galaxies with a stellar mass $M_* > 5\ 10^{10} M_\odot$ are highlighted in red while the others are in orange. The solid lines are the least square fit of the plane, black for the high massive galaxies and grey for the total sample. It can be observed a deviation of the massive groups from the average at redshift between $1 < z < 2$.

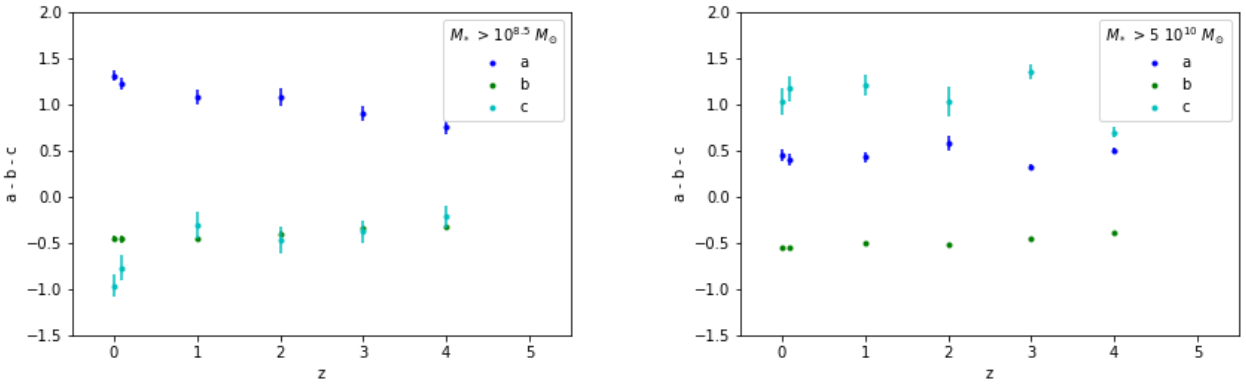


**(a)** **(b)**

**Figure 6:** Here are the displayed the fundamental plane's constants values against redshift. On the left: are the constant values of the total sample. On the right: the constant values for galaxies with a stellar mass $M_* > 5\ 10^{10} M_\odot$.

| z | a | b | c | m | d | scatter |
|---|---|---|---|---|---|---|
| 0 | 1.30 ± 0.06 | -0.46 ± 0.03 | -0.96 ± 0.12 | 0.77 ± 0.05 | 0.16 ± 0.03 | 0.11 |
| 0.1 | 1.22 ± 0.07 | -0.46 ± 0.03 | -0.77 ± 0.14 | 0.76 ± 0.05 | 0.17 ± 0.03 | 0.11 |
| 1 | 1.07 ± 0.09 | -0.46 ± 0.03 | -0.31 ± 0.14 | 0.76 ± 0.06 | 0.13 ± 0.03 | 0.10 |
| 2 | 1.07 ± 0.10 | -0.40 ± 0.02 | -0.47 ± 0.14 | 0.77 ± 0.03 | 0.09 ± 0.01 | 0.08 |
| 3 | 0.90 ± 0.08 | -0.34 ± 0.01 | -0.38 ± 0.12 | 0.86 ± 0.03 | 0.05 ± 0.01 | 0.08 |
| 4 | 0.75 ± 0.08 | -0.32 ± 0.01 | -0.22 ± 0.12 | 0.88 ± 0.02 | 0.04 ± 0.01 | 0.08 |

**Table 3:** Here are the fundamental plane's constants values for the total sample (Fig. 6a). *m*, *d* and *scatter*, are respectively the slope, intercept and scatter of the least square fit.

| z | a | b | c | m | d | scatter |
|---|---|---|---|---|---|---|
| 0 | 0.45 ± 0.06 | -0.55 ± 0.02 | 1.03 ± 0.14 | 0.9 ± 0.05 | 0.07 ± 0.05 | 0.12 |
| 0.1 | 0.40 ± 0.06 | -0.56 ± 0.02 | 1.17 ± 0.14 | 0.88 ± 0.04 | 0.08 ± 0.04 | 0.12 |
| 1 | 0.43 ± 0.05 | -0.50 ± 0.01 | 1.20 ± 0.12 | 0.93 ± 0.04 | 0.04 ± 0.04 | 0.11 |
| 2 | 0.58 ± 0.08 | -0.51 ± 0.01 | 1.03 ± 0.16 | 0.71 ± 0.01 | 0.11 ± 0.01 | 0.07 |
| 3 | 0.32 ± 0.03 | -0.45 ± 0.01 | 1.35 ± 0.08 | 0.86 ± 0.04 | 0.05 ± 0.01 | 0.08 |
| 4 | 0.50 ± 0.02 | -0.40 ± 0.01 | 0.69 ± 0.06 | 0.85 ± 0.01 | -0.02 ± 0.01 | 0.02 |

**Table 4:** Here are the fundamental plane's constants values for galaxies with $M_* > 5\ 10^{10} M_\odot$ (Fig. 6b). *m*, *d* and *scatter*, are respectively the slope, intercept and scatter of the least square fit. (Readers are advised that a $z = 4$ there are less than 5 galaxies with stellar mass $M_* > 5\ 10^{10} M_\odot$.)

## 3.3 Ie - Re plane

The most easily accessible correlation of galaxy parameters at low and high redshift is the $I_e - R_e$ plane, one of the orthogonal projections of the FP, first discovered by Kormendy (1977) [49] for bright ETGs. After new data of faint ETGs and LTGs were available, Capaccioli et al. (1992) [50], found an ample

curvature in the distribution of galaxies on the plane where bright ETGs were separated from the others. This peculiar distribution suggested the existence of two different populations of ETGs, the 'ordinary' and the 'bright', and was used to argue for distinct channels of formation for dwarfs and giants ETGs (see e.g. Capaccioli et al. 1993 [51]; Kormendy et al. 2009 [52]). Graham & Guzmàn 2003 [53] discussed how a distinction, between the spheroidal components with a Sérsic profile and those with a core-Sérsic profile, occurs at magnitude $M_B = -20.5\ mag$, that correspond at a mass of $\sim 2\ 10^{11}\ M_\odot$. This associates the curvature in the $I_e - R_e$ plane with the continuous change of the Sèrsic index ($n$) with luminosity shown in Fig. 1. Another peculiar feature of the plane is the presence of a zone of exclusion (ZoE) at high luminosity and radius (Bender et al. 1992 [54]; Bursten et al. 1997 [55]). This ZoE is defined by the virial theorem its boundary is delimited by a straight line with slope $m = 1$.

In Fig. 7 the $I_e - R_e$ plane is shown at different redshifts. It can be noticed how the massive galaxies always distribute near the ZoE, with slope reported in Tab. 5, while the others have a more scattered distribution and start departure from the ZoE around $z = 1$. This implies that even if the FP has a very small scatter, as seen in Sec. 3.2, the distribution of galaxies on it isn't homogeneous. From Fig. 7 one can appreciate how galaxies were smaller and brighter in the distant past compared to now. As time passed, they aged and expanded with space resulting in a decrease in surface brightness and an increase in radius.

| z | m | d | scatter |
|---|---|---|---|
| 0 | -1.51 ± 0.05 | 3.29 ± 0.05 | 0.16 |
| 1 | -1.81 ± 0.04 | 4.07 ± 0.03 | 0.17 |
| 2 | -1.96 ± 0.03 | 4.46 ± 0.02 | 0.16 |
| 4 | - | - | - |

**Table 5:** Here are reported the values of the slope, intercept and scatter of the least square fit for massive galaxies in the $I_e - R_e$ plane. values at $z = 4$ aren't available because there are less than 5 galaxies with enough stellar mass.

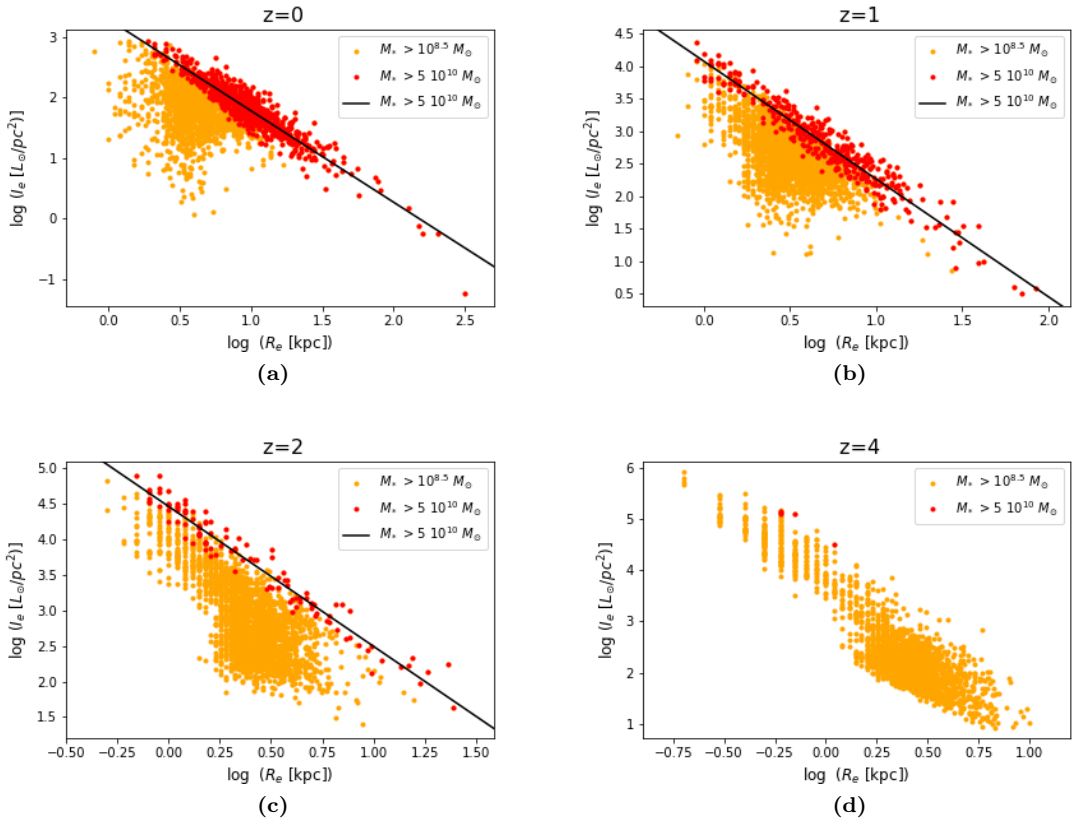


**Figure 7:** Here is displayed the $I_e - R_e$ plane at some different redshifts. Galaxies with a stellar mass $M_* > 5\ 10^{10} M_\odot$ are highlighted in red. The solid line is the least square fit of the massive galaxies.

## 3.4 Faber-Jackson diagram

Another orthogonal projection of the FP is the Faber-Jackson (FJ) plane first observed by Faber & Jackson (1976) [3]. On the FJ, the galaxies distribute with a little scatter around a line, and only in a second moment was observed that bright ETGs follow a steeper slope than the fainter ones (see e.g. Desroches et al. 2007[56]; Choi et al. 2007 [57]; Nigoche-Netro et al. 2011 [58]; D'Onofrio & Chiosi 2022 [59]). This trend isn't reproduced by EAGLE's data which seems to lead to an opposite result as shown in Fig. 8. This effect may be a selection effect caused by the fact that, as described in Sec. 2.2, the galaxy's magnitude has been computed only inside a radius of 30 pkpc. This is obviously too small for large galaxies as the massive ones. In the other diagrams, the surface brightness is considered instead of the simple luminosity as in this case, and it seems that the $L/R^2$ ratio is less influenced by this selection effect as the results of Sec. 3.3 are compatible with observations. Another peculiarity of the FJ plane found with the EAGLE data is the big scatter of the galaxies. The values are reported in Tab. 6 and Tab. 7, where the integrity of the sample and only the massive galaxies were respectively considered.

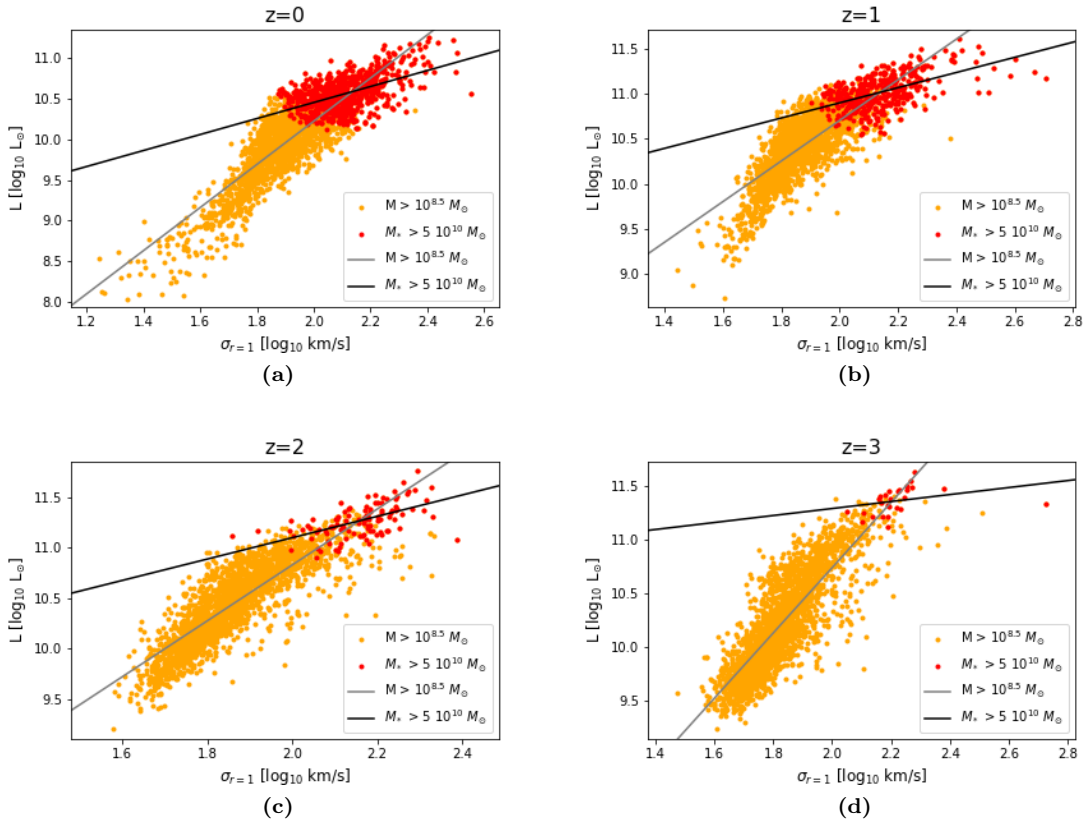


**Figure 8:** Here is displayed the $L - \sigma$ plane at different redshift and galaxies with a stellar mass $M_* > 5\ 10^{10} M_\odot$ are highlighted in red. The black solid line is the least square fit for the massive galaxies, and the grey one is for the total sample

| z | m | d | scatter |
|---|---|---|---|
| 0 | 2.67 ± 0.13 | 4.89 ± 0.25 | 0.25 |
| 1 | 2.26 ± 0.16 | 6.19 ± 0.31 | 0.23 |
| 2 | 2.77 ± 0.15 | 5.29 ± 0.27 | 0.21 |
| 3 | 3.06 ± 0.18 | 4.62 ± 0.33 | 0.25 |

**Table 6:** Here are reported the values of the least square fit on the total sample displayed in Fig. 8.

| z | m | d | scatter |
|---|---|---|---|
| 0 | 1.00 ± 0.14 | 8.46 ± 0.29 | 0.18 |
| 1 | 0.85 ± 0.10 | 9.20 ± 0.21 | 0.16 |
| 2 | 1.07 ± 0.13 | 8.96 ± 0.29 | 0.13 |
| 3 | 0.35 ± 0.14 | 10.58 ± 0.31 | 0.12 |

**Table 7:** Here are reported the values of the least square fit on the galaxies with a stellar mass $M_* > 5\ 10^{10} M_\odot$ displayed in Fig. 8.

## 3.5 Comparison with virial theorem

One of the possible explanations for the fundamental plane tilt proposed in Sec. 1 is the content of dark matter. This idea arises from the virial theorem, where the totality of the galaxy's mass is taken into consideration and not only the stellar one that can be indirectly measured by the luminosity. Then, from the theory, galaxies should be distributed on the plane:

$$logR_t = 2\ log\sigma - \ logI_m \tag{4}$$

where $R_t$ is half of the total mass radius and $I_m$ is the surface mass density defined as:

$$I_m = \frac{M_{tot}}{2\pi R_{tot}^2} \tag{5}$$

As has been discussed before, massive galaxies evolve differently compared to less massive ones, for this reason, in Fig. 9 it is shown the plane of Eq. 4 for galaxies with a stellar mass $M > 10^{10}\ M_\odot$. In this case, the half total mass radius of the entire galaxy wasn't available and then, the half dark matter mass one was utilised instead. One can observe from Tab. 8, how the values of the constants are close to the theoretical ones, and from Tab. 9 how the scatter is low, even considering an under-estimated radius as the one utilised in this case.

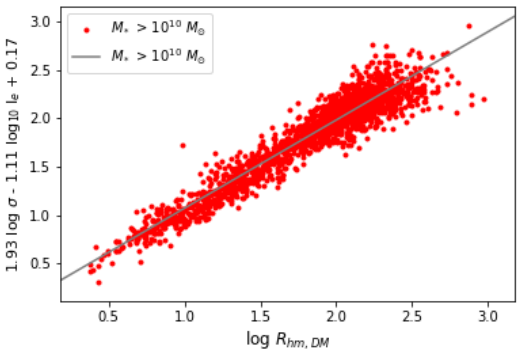


**Figure 9:** Here is displayed the fundamental plane considering, the half dark matter radius and the surface mass density, at $z = 0$ for galaxies with a stellar mass $M > 10^{10}\ M_\odot$.

| | a | b | c |
|---|---|---|---|
| virial theorem | 2 | -1 | 0 |
| EAGLE | 1.93 ± 0.11 | -1.11 ± 0.03 | 0.17 ± 0.23 |

**Table 8:** Theoretical fundamental plane's constant compared to the simulated one considering the half dark matter mass radius at $z = 0$

| m | d | scatter |
|---|---|---|
| 0.91 ± 0.02 | 0.16 ± 0.04 | 0.14 |

**Table 9**

# 4 Conclusion

In this work, it has been roughly studied the evolution of the fundamental plane at different epochs utilising the EAGLE simulation data.

What has been observed is:

i the EAGLE simulation naturally develops non-homological early-type galaxies and they're in good agreement with the observational WINGS data on the $L-n$ plane. While on the $R-n$ plane the simulation doesn't correlate as well with the observed galaxies;

ii the fundamental plane actually evolves with time but the scatter remains pretty small, around $\sim 0.1$, even at high redshift. Indeed, it even seems to reduce at higher redshifts, but this will need to be verified by a more accurate study;

iii high massive galaxies distribute on a different plane compared to the less massive ones starting at redshift $1 < z < 2$, while at higher values of z, it doesn't seem to occur;

iv the EAGLE simulation reproduce quite well the shape of the $I_e - R_e$ plane at low redshifts. It has been seen that massive galaxies evolve along the zone of exclusion whereas the others begin to disperse in a cloud from $z \sim 1$. At this redshift, it has been observed how the typical curvature on the plane, visible at lower value of z, begins to take shape while before it wasn't present;

v the Faber-Jackson plane ($L - \sigma$) for high massive galaxies isn't well reproduced by the EAGLE's data as their slope is less steeper than for the less massive ones. This is probably caused by a selection effect due to the limited portion of the galaxy considered to compute the magnitude;

vi if computing the fundamental plane at $z = 0$, considering the half dark matter radius as an approximation of the half total mass one, and the surface mass density within this radius instead of the mean surface brightness; the EAGLE simulation's data lead to a solution close to the theoretical one with the values of $a = 1.93 \pm 0.11$ and $b = -1.11 \pm 0.03$.

The analysis carried out leads to the conclusion that, in a first approximation, the EAGLE simulation data don't only suggest a time dependence on the fundamental plane's slope, they also propose that massive galaxies depend less on time than the lighter ones. Moreover, the data confirm different trends for the two galaxies category showing how this difference starts at a redshift between $1 < z < 2$. This work isn't meant to give precise results, but only to give a first qualitative appraisal of the dependence on time of the fundamental plane. Therefore, more deeper and accurate studies are needed to verify what has been found in this work.

# 5 Acknowledgment

We acknowledge the Virgo Consortium for making their simulation data available. The eagle simulations were performed using the DiRAC-2 facility at Durham, managed by the ICC, and the PRACE facility Curie based in France at TGCC, CEA, Bruyères-le-Châtel

I would like to personally thank the supervisor D'Onofrio Mauro for letting me work on this project and for always being available for clarifications when needed.

I also would like to thank all the people who have been close to me and supported me over the past few years.

# References


[1] S. Djorgovski and M. Davis, "Fundamental properties of elliptical galaxies," *Astrophysical Journal*, vol. 313, pp. 59–68, 1987.

[2] A. Dressler, D. Lynden-Bell, D. Burstein, R. L. Davies, S. Faber, R. Terlevich, and G. Wegner, "Spectroscopy and photometry of elliptical galaxies. i-a new distance estimator," *Astrophysical Journal, Part 1 (ISSN 0004-637X), vol. 313, Feb. 1, 1987, p. 42-58.*, vol. 313, pp. 42–58, 1987.

[3] R. E. Faber, S. M. ; Jackson, "Velocity dispersions and mass-to-light ratios for elliptical galaxies," *Astrophysical Journal, Vol. 204, p. 668-683*, 1976.

[4] L. Ciotti, "Stellar systems following the r exp 1/m luminosity law," *Astronomy and Astrophysics*, vol. 249, pp. 99–106, 1991.

[5] I. Jørgensen, M. Franx, and P. Kjaergaard, "The fundamental plane for cluster e and s0 galaxies," *Monthly Notices of the Royal Astronomical Society*, vol. 280, no. 1, pp. 167–185, 1996.

[6] M. Cappellari, R. Bacon, M. Bureau, M. Damen, R. L. Davies, P. T. De Zeeuw, E. Emsellem, J. Falcón-Barroso, D. Krajnovic, H. Kuntschner *et al.*, "The sauron project—iv. the mass-to-light ratio, the virial mass estimator and the fundamental plane of elliptical and lenticular galaxies," *Monthly Notices of the Royal Astronomical Society*, vol. 366, no. 4, pp. 1126–1150, 2006.

[7] M. D'onofrio, T. Valentinuzzi, L. Secco, R. Caimmi, and D. Bindoni, "Toward understanding the origin of the fundamental plane for early-type galaxies," *New Astronomy Reviews*, vol. 50, no. 6, pp. 447–460, 2006.

[8] A. S. Bolton, S. Burles, T. Treu, L. V. Koopmans, and L. A. Moustakas, "A more fundamental plane," *The Astrophysical Journal*, vol. 665, no. 2, p. L105, 2007.

[9] P. Prugniel and F. Simien, "The fundamental plane of early-type galaxies: non-homology of the spatial structure." *Astronomy and Astrophysics, v. 321, p. 111-122*, vol. 321, pp. 111–122, 1997.

[10] E. Brocato, M. Capaccioli, and M. Condelli, "Surface brightness fluctuations as distance indicators: a new approach based on population synthesis models," *Memorie della Società Astronomia Italiana, Vol. 69, p. 155*, vol. 69, p. 155, 1998.

[11] I. Trujillo, A. Burkert, and E. F. Bell, "The tilt of the fundamental plane: Three-quarters structural nonhomology, one-quarter stellar population," *The Astrophysical Journal*, vol. 600, no. 1, p. L39, 2003.

[12] M. D'Onofrio, G. Fasano, J. Varela, D. Bettoni, M. Moles, P. Kjærgaard, E. Pignatelli, B. Poggianti, A. Dressler, A. Cava *et al.*, "The fundamental plane of early-type galaxies in nearby clusters from the wings database," *The Astrophysical Journal*, vol. 685, no. 2, p. 875, 2008.

[13] P. G. v. Dokkum and M. Franx, "The fundamental plane in cl 0024 at z= 0.4: implications for the evolution of the mass-to-light ratio," *Monthly Notices of the Royal Astronomical Society*, vol. 281, no. 3, pp. 985–1000, 1996.

[14] B. P. Holden, A. van der Wel, D. D. Kelson, M. Franx, and G. D. Illingworth, "M/lb and color evolution for a deep sample of m cluster galaxies at z 1: The formation epoch and the tilt of the fundamental plane," *The Astrophysical Journal*, vol. 724, no. 1, p. 714, 2010.

[15] A. De Graaff, R. Bezanson, M. Franx, A. van der Wel, B. Holden, J. van de Sande, E. F. Bell, F. D'Eugenio, M. V. Maseda, A. Muzzin *et al.*, "The fundamental plane in the lega-c survey: Unraveling the m/l ratio variations of massive star-forming and quiescent galaxies at z 0.8," *The Astrophysical Journal*, vol. 913, no. 2, p. 103, 2021.

[16] L. Ciotti, B. Lanzoni, and A. Renzini, "The tilt of the fundamental plane of elliptical galaxies—i. exploring dynamical and structural effects," *Monthly Notices of the Royal Astronomical Society*, vol. 282, no. 1, pp. 1–12, 1996.

[17] A. Borriello, P. Salucci, and L. Danese, "The fundamental plane of ellipticals—i. the dark matter connection," *Monthly Notices of the Royal Astronomical Society*, vol. 341, no. 4, pp. 1109–1120, 2003.

[18] C. Tortora, N. Napolitano, A. J. Romanowsky, M. Capaccioli, and G. Covone, "Central mass-to-light ratios and dark matter fractions in early-type galaxies," *Monthly Notices of the Royal Astronomical Society*, vol. 396, no. 2, pp. 1132–1150, 2009.

[19] D. Zaritsky, A. H. Gonzalez, and A. I. Zabludoff, "The fundamental manifold of spheroids," *The Astrophysical Journal*, vol. 638, no. 2, p. 725, 2006.

[20] J. B. Hyde and M. Bernardi, "The luminosity and stellar mass fundamental plane of early-type galaxies," *Monthly Notices of the Royal Astronomical Society*, vol. 396, no. 2, pp. 1171–1185, 2009.

[21] Y. Yoon and C. Park, "The fundamental plane is not a plane: Warped nature of the fundamental plane of early-type galaxies and its implication for galaxy formation," *The Astrophysical Journal*, vol. 936, no. 1, p. 22, aug 2022. [Online]. Available: https://dx.doi.org/10.3847/1538-4357/ac854a

[22] M. D'Onofrio, M. Capaccioli, S. R. Zaggia, and N. Caon, "The relative distances to the virgo, fornax and coma clusters of galaxies through the dn-$\sigma$ and the fundamental plane relations," *Monthly Notices of the Royal Astronomical Society*, vol. 289, no. 4, pp. 847–862, 1997.

[23] P. G. Van Dokkum and R. P. Van der Marel, "The star formation epoch of the most massive early-type galaxies," *The Astrophysical Journal*, vol. 655, no. 1, p. 30, 2007.

[24] J. A. Willick, S. Courteau, S. M. Faber, D. Burstein, and A. Dekel, "Homogeneous velocity-distance data for peculiar velocity analysis. i. calibration of cluster samples," *arXiv preprint astro-ph/9411046*, 1994.

[25] M. A. Strauss and J. A. Willick, "The density and peculiar velocity fields of nearby galaxies," *Physics reports*, vol. 261, no. 5-6, pp. 271–431, 1995.

[26] J. Schaye, R. A. Crain, R. G. Bower, M. Furlong, M. Schaller, T. Theuns, C. Dalla Vecchia, C. S. Frenk, I. G. McCarthy, J. C. Helly, A. Jenkins, Y. M. Rosas-Guevara, S. D. M. White, M. Baes, C. M. Booth, P. Camps, J. F. Navarro, Y. Qu, A. Rahmati, T. Sawala, P. A. Thomas, and J. Trayford, "The EAGLE project: simulating the evolution and assembly of galaxies and their environments," *Monthly Notices of the Royal Astronomical Society*, vol. 446, no. 1, pp. 521–554, 11 2014. [Online]. Available: https://doi.org/10.1093/mnras/stu2058

[27] R. A. Crain, J. Schaye, R. G. Bower, M. Furlong, M. Schaller, T. Theuns, C. Dalla Vecchia, C. S. Frenk, I. G. McCarthy, J. C. Helly, A. Jenkins, Y. M. Rosas-Guevara, S. D. M. White, and J. W. Trayford, "The EAGLE simulations of galaxy formation: calibration of subgrid physics and model variations," , vol. 450, no. 2, pp. 1937–1961, Jun. 2015.

[28] A. Jenkins, "Second-order lagrangian perturbation theory initial conditions for resimulations," *Monthly Notices of the Royal Astronomical Society*, vol. 403, no. 4, pp. 1859–1872, 2010.

[29] V. Springel, "The cosmological simulation code gadget-2," *Monthly notices of the royal astronomical society*, vol. 364, no. 4, pp. 1105–1134, 2005.

[30] R. P. Wiersma, J. Schaye, and B. D. Smith, "The effect of photoionization on the cooling rates of enriched, astrophysical plasmas," *Monthly Notices of the Royal Astronomical Society*, vol. 393, no. 1, pp. 99–107, 2009.

[31] J. Schaye and C. Dalla Vecchia, "On the relation between the schmidt and kennicutt–schmidt star formation laws and its implications for numerical simulations," *Monthly Notices of the Royal Astronomical Society*, vol. 383, no. 3, pp. 1210–1222, 2008.

[32] R. P. Wiersma, J. Schaye, T. Theuns, C. Dalla Vecchia, and L. Tornatore, "Chemical enrichment in cosmological, smoothed particle hydrodynamics simulations," *Monthly Notices of the Royal Astronomical Society*, vol. 399, no. 2, pp. 574–600, 2009.

[33] C. Dalla Vecchia and J. Schaye, "Simulating galactic outflows with thermal supernova feedback," *Monthly Notices of the Royal Astronomical Society*, vol. 426, no. 1, pp. 140–158, 2012.

[34] Y. M. Rosas-Guevara, R. G. Bower, J. Schaye, M. Furlong, C. S. Frenk, C. M. Booth, R. A. Crain, C. Dalla Vecchia, M. Schaller, and T. Theuns, "The impact of angular momentum on black hole accretion rates in simulations of galaxy formation," *Monthly Notices of the Royal Astronomical Society*, vol. 454, no. 1, p. 1038–1057, Sep. 2015. [Online]. Available: http://dx.doi.org/10.1093/mnras/stv2056

[35] S. McAlpine, J. C. Helly, M. Schaller, J. W. Trayford, Y. Qu, M. Furlong, R. G. Bower, R. A. Crain, J. Schaye, T. Theuns *et al.*, "The eagle simulations of galaxy formation: Public release of halo and galaxy catalogues," *Astronomy and Computing*, vol. 15, pp. 72–89, 2016.

[36] V. Springel, S. D. White, G. Tormen, and G. Kauffmann, "Populating a cluster of galaxies–i. results at z= 0," *Monthly Notices of the Royal Astronomical Society*, vol. 328, no. 3, pp. 726–750, 2001.

[37] K. Dolag, S. Borgani, G. Murante, and V. Springel, "Substructures in hydrodynamical cluster simulations," *Monthly Notices of the Royal Astronomical Society*, vol. 399, no. 2, pp. 497–514, 2009.

[38] M. Davis, G. Efstathiou, C. S. Frenk, and S. D. White, "The evolution of large-scale structure in a universe dominated by cold dark matter," *Astrophysical Journal, Part 1 (ISSN 0004-637X), vol. 292, May 15, 1985, p. 371-394. Research supported by the Science and Engineering Research Council of England and NASA.*, vol. 292, pp. 371–394, 1985.

[39] J. P. Naiman, A. Pillepich, V. Springel, E. Ramirez-Ruiz, P. Torrey, M. Vogelsberger, R. Pakmor, D. Nelson, F. Marinacci, L. Hernquist, R. Weinberger, and S. Genel, "First results from the illustristng simulations: a tale of two elements – chemical evolution of magnesium and europium," *Monthly Notices of the Royal Astronomical Society*, vol. 477, no. 1, p. 1206–1224, Mar. 2018. [Online]. Available: http://dx.doi.org/10.1093/mnras/sty618

[40] V. Springel, R. Pakmor, A. Pillepich, R. Weinberger, D. Nelson, L. Hernquist, M. Vogelsberger, S. Genel, P. Torrey, F. Marinacci, and J. Naiman, "First results from the illustristng simulations: matter and galaxy clustering," *Monthly Notices of the Royal Astronomical Society*, vol. 475, no. 1, p. 676–698, Dec. 2017. [Online]. Available: http://dx.doi.org/10.1093/mnras/stx3304

[41] F. Marinacci, M. Vogelsberger, R. Pakmor, P. Torrey, V. Springel, L. Hernquist, D. Nelson, R. Weinberger, A. Pillepich, J. Naiman, and S. Genel, "First results from the illustristng simulations: radio haloes and magnetic fields," *Monthly Notices of the Royal Astronomical Society*, Aug. 2018. [Online]. Available: http://dx.doi.org/10.1093/mnras/sty2206

[42] A. Pillepich, D. Nelson, L. Hernquist, V. Springel, R. Pakmor, P. Torrey, R. Weinberger, S. Genel, J. P. Naiman, F. Marinacci, and M. Vogelsberger, "First results from the illustristng simulations: the stellar mass content of groups and clusters of galaxies," *Monthly Notices of the Royal Astronomical Society*, vol. 475, no. 1, p. 648–675, Dec. 2017. [Online]. Available: http://dx.doi.org/10.1093/mnras/stx3112

[43] D. Nelson, A. Pillepich, V. Springel, R. Weinberger, L. Hernquist, R. Pakmor, S. Genel, P. Torrey, M. Vogelsberger, G. Kauffmann, F. Marinacci, and J. Naiman, "First results from the illustristng simulations: the galaxy colour bimodality," *Monthly Notices of the Royal Astronomical Society*, vol. 475, no. 1, p. 624–647, Nov. 2017. [Online]. Available: http://dx.doi.org/10.1093/mnras/stx3040

[44] A. de Graaff, J. Trayford, M. Franx, M. Schaller, J. Schaye, and A. van der Wel, "Observed structural parameters of EAGLE galaxies: reconciling the mass–size relation in simulations with local observations," *Monthly Notices*

*of the Royal Astronomical Society*, vol. 511, no. 2, pp. 2544–2564, 12 2021. [Online]. Available: https://doi.org/10.1093/mnras/stab3510

[45] A. de Graaff, M. Franx, E. F. Bell, R. Bezanson, M. Schaller, J. Schaye, and A. van der Wel, "A common origin for the fundamental plane of quiescent and star-forming galaxies in the EAGLE simulations," *Monthly Notices of the Royal Astronomical Society*, vol. 518, no. 4, pp. 5376–5402, 11 2022. [Online]. Available: https://doi.org/10.1093/mnras/stac3277

[46] C. N. A. Willmer, "The absolute magnitude of the sun in several filters," *The Astrophysical Journal Supplement Series*, vol. 236, no. 2, p. 47, Jun. 2018. [Online]. Available: http://dx.doi.org/10.3847/1538-4365/aabfdf

[47] I. Strateva, Ivezić, G. R. Knapp, V. K. Narayanan, M. A. Strauss, J. E. Gunn, R. H. Lupton, D. Schlegel, N. A. Bahcall, J. Brinkmann, R. J. Brunner, T. Budavári, I. Csabai, F. J. Castander, M. Doi, M. Fukugita, Z. Győry, M. Hamabe, G. Hennessy, T. Ichikawa, P. Z. Kunszt, D. Q. Lamb, T. A. McKay, S. Okamura, J. Racusin, M. Sekiguchi, D. P. Schneider, K. Shimasaku, and D. York, "Color separation of galaxy types in the sloan digital sky survey imaging data," *The Astronomical Journal*, vol. 122, no. 4, p. 1861–1874, Oct. 2001. [Online]. Available: http://dx.doi.org/10.1086/323301

[48] S. di Serego Alighieri and B. Lanzoni, "Mass and environment drive the evolution of early-type galaxies," 2006.

[49] J. Kormendy, "Brightness distributions in compact and normal galaxies. ii-structure parameters of the spheroidal component," *Astrophysical Journal, Part 1, vol. 218, Dec. 1, 1977, p. 333-346. Research supported by the California Institute of Technology and National Research Council of Canada.*, vol. 218, pp. 333–346, 1977.

[50] M. Capaccioli, N. Caon, and M. D'Onofrio, "Families of galaxies in the $\mu$ e–r e plane," *Monthly Notices of the Royal Astronomical Society*, vol. 259, no. 2, pp. 323–327, 1992.

[51] M. Capaccioli, N. Caon, M. D'Onofrio *et al.*, "The (log re, $\mu$e) plane of hot stellar systems," in *Structure, Dynamics and Chemical Evolution of Elliptical Galaxies*. I. John Danziger, WW Zeilinger, and Kurt Kjaer,, 1993, p. 43.

[52] J. Kormendy, D. B. Fisher, M. E. Cornell, and R. Bender, "Structure and formation of elliptical and spheroidal galaxies," *The Astrophysical Journal Supplement Series*, vol. 182, no. 1, p. 216, 2009.

[53] A. W. Graham and R. Guzmán, "Hst photometry of dwarf elliptical galaxies in coma, and an explanation for the alleged structural dichotomy between dwarf and bright elliptical galaxies," *The Astronomical Journal*, vol. 125, no. 6, p. 2936, 2003.

[54] R. Bender, D. Burstein, and S. Faber, "Dynamically hot galaxies. i-structural properties," *Astrophysical Journal, Part 1 (ISSN 0004-637X), vol. 399, no. 2, p. 462-477.*, vol. 399, pp. 462–477, 1992.

[55] D. Burstein, R. Bender, S. Faber, and R. Nolthenius, "Global relationships among the physical properties of stellar systems," *arXiv preprint astro-ph/9707037*, 1997.

[56] L.-B. Desroches, E. Quataert, C.-P. Ma, and A. A. West, "Luminosity dependence in the fundamental plane projections of elliptical galaxies," *Monthly Notices of the Royal Astronomical Society*, vol. 377, no. 1, p. 402–414, May 2007. [Online]. Available: http://dx.doi.org/10.1111/j.1365-2966.2007.11612.x

[57] Y. Choi, C. Park, and M. S. Vogeley, "Internal and collective properties of galaxies in the sloan digital sky survey," *The Astrophysical Journal*, vol. 658, no. 2, p. 884–897, Apr. 2007. [Online]. Available: http://dx.doi.org/10.1086/511060

[58] Nigoche-Netro, A., Aguerri, J. A. L., Lagos, P., Ruelas-Mayorga, A., Sánchez, L. J., Muñoz-Tuñón, C., and Machado, A., "The intrinsic dispersion in the faber-jackson relation for early-type galaxies as function of the mass and redshift," *AA*, vol. 534, p. A61, 2011. [Online]. Available: https://doi.org/10.1051/0004-6361/201016360

[59] M. D'Onofrio and C. Chiosi, "Tomography of the ie-re and l-sigma planes," *Universe*, vol. 8, no. 1, 2022. [Online]. Available: https://www.mdpi.com/2218-1997/8/1/8